PASSIVE FAULT TOLERANT CONTROL OF A DUAL-SYSTEM UAV IN TRANSITION FLIGHT

Junfeng Cai[1] & Marco Lovera[1]

[1]Department of Aerospace Science and Technology, Politecnico di Milano, Italy

Abstract

A novel passive fault tolerant control system for the transition flight of a dual-system UAV is proposed in this paper. The nominal control synthesis is firstly conducted without considering the occurrence of actuator fault. Stability evaluation using μ-analysis and performance analysis based on a multi-model approach, by assuming the existence of actuator fault, are subsequently carried out, which suggests the nominal control system can maintain stability and performance under partial loss of a single propeller. To further illustrate the effectiveness of passive fault tolerance and the robustness to modeling uncertainty of the proposed control system, validation on the nonlinear six-degree-of-freedom simulator is carried out. The simulation results show that the developed control system using structured H_∞ is able to overcome the partial loss of a single propeller as well as modeling uncertainty during transition flight, which improves the safety and reliability of the flight of the dual system UAV.

Keywords: Fault Tolerant Control, Transition Flight, Structured H_∞, Dual-System UAV

1. Introduction

Unmanned aerial vehicles (UAVs) are drawing growing attention due to their application to an increasing number of fields. In particular, vertical take-off and landing (VTOL) UAVs have become the focus of the researchers in recent years. Compared to fixed wing UAVs, VTOL UAVs are capable of vertically taking off and landing without runway. In terms of power efficiency, VTOL UAVs possess lower power consumption than multicopter UAVs that enables a much longer flight range with the same battery capacity. VTOL UAVs can be divided into several types [1], such as the tilt rotor UAV, the tail-sitter UAV and the dual-system UAV. The tilt rotor UAV involves a tilting mechanism of the propellers which usually leads to a more complicated mechanical structure. For the tail-sitter UAV, it takes off on its tail then undergoes an attitude transition from vertical direction to horizontal direction. This significant attitude change constraints its application. To this effect, the dual-system UAV is favored in this paper since it has a relatively simple mechanical structure and can ensure a smooth transition process without large attitude variations, which makes it suitable for potential applications like logistics.

For the hybrid VTOL UAV, the design of control laws for transition flight is the main challenge. It is because the complexity of the aerodynamic modeling resulting from the interaction between the rotors and wing that further results in the uncertainty of the dynamic model. In [2], a nonlinear robust controller was designed for the flight transition process of a tail-sitter aircraft, which is composed of a nominal H_∞ controller and a nonlinear disturbance observer. In [3], a transition flight controller was proposed employing adaptive neural network dynamic inversion for the Canard Rotor/Wing UAV by simplifying the transition process to the longitudinal plane and the performance of the attitude control loop and trajectory control loop were evaluated. In [4], an incremental nonlinear dynamic inversion controller based on quadratic programming control allocation was developed for a dual-system eVTOL. However, the existing research work suffers from some disadvantages and limitations. For the existing transition control methods proposed for hybrid VTOL UAVs, there is no involvement of the

possible occurrence of actuator faults. The fault tolerance capability of these developed controllers is unknown. Moreover, in [3] and [4], the design of the transition flight controller is based on the simplified model in longitudinal plane that limits the scope of the discussion of aircraft motion only in longitudinal plane, where the lateral and directional motion control is not considered.

The front transition flight of the dual-system UAV from multicopter mode to fixed wing mode is a critical flight phase. If any actuator fault or failure occurs during this process it will be a big threat to the flight safety. On the other hand, the dual-system UAV has the feature of actuators redundancy which provides the possibility for the development of fault tolerant control (FTC) capability. FTC can be separated into active FTC and passive FTC. Active FTC reacts to the occurred faults in time by changing the control system accordingly. It usually includes a fault detection and diagnosis module for providing fault information in real time. In contrast, passive FTC consists in designing controllers that are robust to certain faults without the need for fault information. With specific focus on Hybrid VTOL UAVs, there have been some existing research results regarding FTC. In [5], an adaptive fault-tolerant control scheme for the hybrid Canard Rotor/Wing UAV was presented. The adaptive sliding mode controller can compensate the virtual control signal error caused by actuator faults by adjusting control parameters. In [6], an integral sliding mode-based model reference control law is employed to design the FTC scheme for the fixed-wing mode of a dual-system UAV. The methodology of incremental nonlinear dynamic inversion combined with adaptive sliding mode control was applied to a Quad-plane aircraft in [7] and the capability of the proposed method for tolerating a complete rotor loss in multicopter mode was also discussed. The fault tolerant control of hybrid VTOL UAVs in transition flight still needs to be further investigated.

Structured H_∞ as a control synthesis method to obtain the parameters of a pre-defined control architecture that is capable of coping with system uncertainties has been applied in the FTC of aerospace systems. A FTC approach for multicopter UAVs based on gain-scheduling control using structured H_∞ synthesis with multi-models was reported in [8]. In [9], classical root locus and structured H_∞ designs are compared for the longitudinal control law of a civil aircraft considering model uncertainties and actuator faults. A fault detection and isolation (FDI) algorithm was developed to provide fault information for control law switching in a multi-model approach for a high-altitude, long-endurance aircraft, where structured H_∞ is applied to the switching control laws design [10]. A helicopter rotor-state feedback control law based on structured H_∞ was proposed with the fault tolerance of the failure of rotor state sensors, whereas, without considering the situation of actuator faults [11]. Structured H_∞ already has some successful applications in aerial vehicles. It is interesting to examine its applicability to dual-system UAVs.

In this paper, a transition flight controller for dual-system UAVs is designed using structured H_∞ including the attitude and altitude control of the transition flight phase. Then the stability and performance under actuator fault of the developed control system is analyzed, where the stability analysis is based on μ-analysis and performance evaluation resorts to the perturbed sensitivity function and the corresponding time-domain response in the framework of multi-model. Finally, the effectiveness of FTC of the developed control system subjected to partial loss of one propeller is validated on the nonlinear simulator in the Matlab-Simulink environment.

The paper is organized as follows. Section 2 introduces the dynamic model for transition flight of the dual-system UAV. The structured H_∞ control synthesis for the nominal control system is detailed in Section 3. Section 4 involves the stability and performance analysis of the designed control system given that there is occurrence of fault in single propeller. Section 5 reports the simulation results under fault scenarios on the nonlinear simulator. Section 6 concludes the paper.

2. Problem Formulation

Our research object is the dual-system UAV that has a hybrid configuration with eight vertical propellers, two horizontal propellers, fixed wing, elevator, ailerons and rudders. The schematic is shown in Figure 1. When the drone is in multicopter mode only vertical propellers keep working. During the fixed-wing mode, only horizontal propellers and control surfaces are working such that the drone can fly as a fixed-wing aircraft. Whereas, all the actuators are activated when it is in transition flight phase.

2.1 Equations of Motion

The mathematical model of the dual-system UAV is expressed in body-fixed axes denoted as (o_b, x_b, y_b, z_b), where o_b is the origin of the body-fixed axes that coincides with the center of gravity of the aircraft. Since during transition flight we assume the aircraft keeps steady level flight without any manoeuvre, it is assumed that the altitude remains constant. So we focus on the attitude dynamics and the position dynamics in z axis. Furthermore, since the transition flight from multicopter mode to fixed-wing mode usually lasts a few seconds, horizontal position control is not the main concern of this paper. According to the Newton-Euler formulation, the attitude dynamics and the vertical position dynamics of the dual-system UAV in body-fixed axes can be written as follows:

$$\begin{aligned}
\dot{w} &= \frac{F_z}{m} - pv + qu \\
\dot{p} &= \frac{M_x - \dot{r}J_{xz} + qr(J_z - J_y) + qpJ_{xz}}{J_x} \\
\dot{q} &= \frac{M_y - pr(J_x - J_z) - (p^2 - r^2)J_{xz}}{J_y} \\
\dot{r} &= \frac{M_z + \dot{p}J_{xz} - pq(J_y - J_x) - qrJ_{xz}}{J_z}
\end{aligned} \tag{1}$$

where m is the mass of the dual-system UAV, F_z is the resultant force in z direction, M_x, M_y, M_z are the body components of the resultant moment, p, q, r are the body components of the angular rate of the aircraft, J_x, J_y, J_z are inertia moments around the body-fixed axes, J_{xz} is the product of inertia.

2.2 Forces and Moments

The model of the transition flight is complicated by aerodynamic interaction between rotors and wing. However, in view of the satisfying research results obtained in [12] and [4] based on neglecting the aerodynamic coupling , in this paper the aerodynamic coupling is not considered in the modeling. Therefore, the resultant forces and moments presented in Eq. (1) are written as:

$$\begin{aligned}
F_z &= qSC_Z - F_{1a} - F_{1b} - F_{2a} - F_{2b} - F_{3a} - F_{3b} - F_{4a} - F_{4b} + mg\cos\phi\cos\theta \\
M_x &= qSbC_L + F_{1a}l_f + F_{1b}l_f - F_{2a}l_f - F_{2b}l_f - F_{3a}l_r - F_{3b}l_r + F_{4a}l_r + F_{4b}l_r \\
M_y &= qS\bar{c}C_M + F_{1a}l_1 + F_{1b}l_2 + F_{2a}l_1 + F_{2b}l_2 - F_{3a}l_3 - F_{3b}l_4 - F_{4a}l_3 - F_{4b}l_4 \\
M_z &= qSbC_N - M_{1a} + M_{1b} + M_{2a} - M_{2b} + M_{3a} - M_{3b} - M_{4a} + M_{4b}
\end{aligned} \tag{2}$$

where $q = \frac{1}{2}\rho v^2$ is the dynamic pressure, ρ is the air density, v is the airspeed of the UAV, g is the gravitational acceleration, ϕ, θ are respectively roll angle and pitch angle, S denotes wing area, b is wing span, $\bar{c}$ represents mean aerodynamic chord, C_Z is the coefficient of z component of the aerodynamic force in body axes, C_L, C_M, C_N are the coefficients of x, y, z components of the aerodynamic moment in body axes, $l_1, l_2, l_3, l_4, l_r, l_f$ are dimensions of the position of vertical propellers shown in Fig. 1. $F_{ia}, F_{ib}, M_{ia}, M_{ib} (i = 1,2,3,4)$ are forces and moments generated by vertical propellers.
Furthermore, aerodynamic coefficients can be expressed as:

$$\begin{aligned}
C_Z &= C_{Z_0} + C_{Z_\alpha}\alpha + C_{Z_q}q + C_{Z_{\delta_e}}\delta_e \\
C_L &= C_{L_0} + C_{L_\beta}\beta + C_{L_p}p + C_{L_{\delta_a}}\delta_a \\
C_M &= C_{M_0} + C_{M_\alpha}\alpha + C_{M_q}q + C_{M_{\delta_e}}\delta_e \\
C_N &= C_{N_0} + C_{N_\beta}\beta + C_{N_r}r + C_{N_{\delta_r}}\delta_r
\end{aligned} \tag{3}$$

where α is angle of attack, β is sideslip angle, δ_a, δ_e, δ_r are respectively the deflection angle of ailerons, elevator and rudders. Substituting Eq. (3) into (2), it is noticed that the terms that are related to the control forces and moments produced by actuators can be picked out as follows:

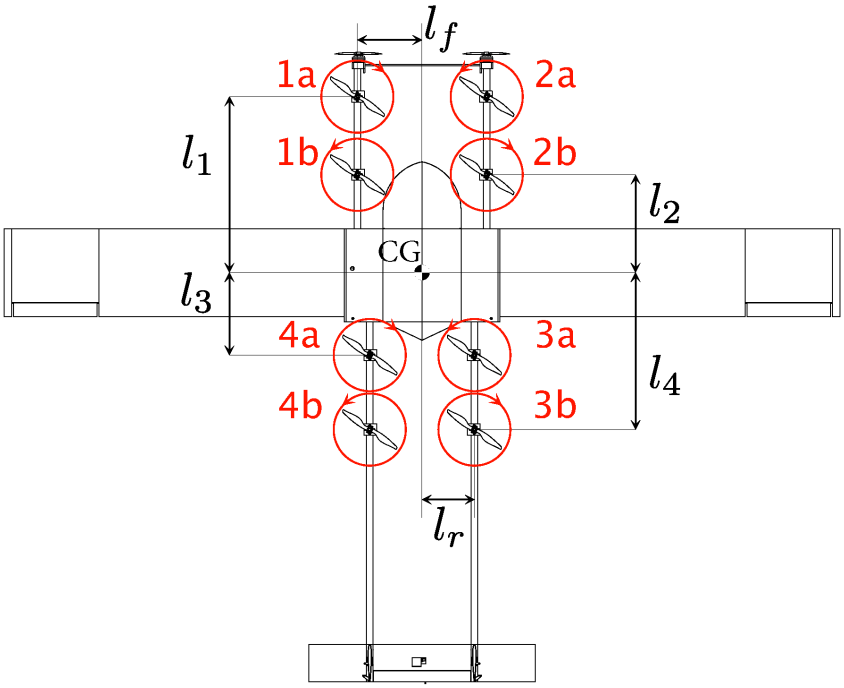

Figure 1 – The top view of the dual-system UAV.

$$
\begin{aligned}
F_{a_z} &= qSC_{Z_{\delta_e}}\delta_e - F_{1a} - F_{1b} - F_{2a} - F_{2b} - F_{3a} - F_{3b} - F_{4a} - F_{4b} \\
M_{a_x} &= qSbC_{L_{\delta_a}}\delta_a + F_{1a}l_f + F_{1b}l_f - F_{2a}l_f - F_{2b}l_f - F_{3a}l_r - F_{3b}l_r + F_{4a}l_r + F_{4b}l_r \\
M_{a_y} &= qS\bar{c}C_{M_{\delta_e}}\delta_e + F_{1a}l_1 + F_{1b}l_2 + F_{2a}l_1 + F_{2b}l_2 - F_{3a}l_3 - F_{3b}l_4 - F_{4a}l_3 - F_{4b}l_4 \\
M_{a_z} &= qSbC_{N_{\delta_r}}\delta_r - M_{1a} + M_{1b} + M_{2a} - M_{2b} + M_{3a} - M_{3b} - M_{4a} + M_{4b}
\end{aligned}
\tag{4}
$$

Note that the term $qSC_{Z_{\delta_e}}\delta_e$ that is the aerodynamic force induced by elevator is very small compared to the other terms such that it is usually neglected.

2.3 Model of the Actuators

The aforementioned forces and moments generated by the propellers $F_{ia}, F_{ib}, M_{ia}, M_{ib}(i = 1,2,3,4)$ are constant times the square of the angular speed. And angular speed is approximately proportional to the throttle percentage. The relationship between the force and moment produced by the single propeller and the commanded throttle can be given by:

$$
\begin{aligned}
F_{i*} &= k_T \cdot Thr_{i*} \\
M_{i*} &= k_M \cdot Thr_{i*}
\end{aligned}
\tag{5}
$$

where the subscript $*$ denotes a or b. Thr_{i*} is the commanded throttle percentage, k_T, k_M are coefficients that are obtained through the calculation of the identification results of the propeller dynamics. In this research, k_T = 0.164 N/%, k_M = 1.89 $\times$ 10^{-3} (N· m)/%. According to Eq. (4), the forces and moments provided by actuators can be rewritten in matrix form:

$$
[F_{a_z}\ M_{a_x}\ M_{a_y}\ M_{a_z}]^T = B[Thr_{1a}\ Thr_{1b}\ Thr_{2a}\ Thr_{2b}\ Thr_{3a}\ Thr_{3b}\ Thr_{4a}\ Thr_{4b}\ \delta_a\ \delta_e\ \delta_r]^T \tag{6}
$$

Subject to constraints: $Thr_{i*} \in [0,\ 100]$, $\delta_a \in [-0.55,\ 0.55]$, $\delta_e \in [-0.5,\ 0.5]$, $\delta_r \in [-0.69,\ 0.69]$. where

$$
B = \begin{bmatrix}
-k_T & -k_T & -k_T & -k_T & -k_T & -k_T & -k_T & -k_T & 0 & 0 & 0 \\
k_T l_f & k_T l_f & -k_T l_f & -k_T l_f & -k_T l_f & -k_T l_f & k_T l_f & k_T l_f & qSlC_{L_{\delta_a}} & 0 & 0 \\
k_T l_1 & k_T l_2 & k_T l_1 & k_T l_2 & -k_T l_3 & -k_T l_4 & -k_T l_3 & -k_T l_4 & 0 & qS\bar{c}C_{M_{\delta_e}} & 0 \\
-k_M & k_M & k_M & -k_M & k_M & -k_M & -k_M & k_M & 0 & 0 & qSbC_{N_{\delta_r}}
\end{bmatrix}. \tag{7}
$$

2.4 Control Allocation

The control allocation problem consists in solving Eq. (6) for the actuator commands satisfying the specified constraints. But there exist a situation that the solutions which satisfy the equation as well as constraints do not exist. In this case, it leads to the following weighted least squares problem:

$$min(\|W_1(u-u_d)\|^2+\gamma\|W_2(Bu-v)\|^2),\quad u_{min}\leq u\leq u_{max} \tag{8}$$

where v denotes the control signal required by the controller. u is the actuator commands. Here $v=[F_{a_z}\ M_{a_x}\ M_{a_y}\ M_{a_z}]^T$, $u=[Thr_{1a}\ Thr_{1b}\ Thr_{2a}\ Thr_{2b}\ Thr_{3a}\ Thr_{3b}\ Thr_{4a}\ Thr_{4b}\ \delta_a\ \delta_e\ \delta_r]^T$, B is the control effectiveness matrix given in (7). u_d is the desired control effort. W_1, W_2 are weighting matrices. $\gamma \gg 1$ such that the second term in Eq. (8) is the dominant term to be optimized. This quadratic programming-based optimization problem can be dealt with the active set method [14] that is able to obtain the optimal solution in a finite number of iterations.

3. Structured H_∞ Control Design for transition

3.1 Control-oriented Model

The equations of motion given in (1) are nonlinear and strongly coupled and are usually employed in the implementation of the six-degree-of-freedom simulator. However, in this section a simplified control-oriented model will be introduced that is more suitable for control design. As already mentioned previously, the transition flight from the multicopter mode to the fixed wing mode is a constant altitude steady level flight. Thus, the variables related to the lateral and directional motion and the attitude angles are very small values such that the corresponding terms can be neglected. Note that the aerodynamic forces and moments in Eq. (2) are regarded as equivalent disturbances. Also, if we consider possible fault caused by actuators it may lead to the loss of the control force and moments effectiveness denoted as $\Gamma=[\gamma_T\ \gamma_L\ \gamma_M\ \gamma_N]$. Then Eq. (1) can be simplified and rearranged as follows:

$$\begin{aligned}\dot{w}&=\frac{(1-\gamma_T)F_z}{m}\\ \dot{p}&=\frac{(1-\gamma_L)M_x}{J_x}\\ \dot{q}&=\frac{(1-\gamma_M)M_y}{J_y}\\ \dot{r}&=\frac{(1-\gamma_N)M_z}{J_z}\end{aligned} \tag{9}$$

where the possible range of Γ is calculated according to the assumed actuator fault. Here the maximum loss of effectiveness of a single vertical propeller is assumed to be 60%. The resulting loss of the control force and moments caused by the assumed fault is thereby calculated with $\gamma_T=\Delta T/\bar{T}$, $\gamma_L=\Delta L/\bar{L}$, $\gamma_M=\Delta M/\bar{M}$, $\gamma_N=\Delta N/\bar{N}$, the values of which are respectively 0.3, 0.2, 0.2, 0.05. Where ΔT, ΔL, ΔM, ΔN are respectively increment of the control force and control moments along o_bx_b, o_by_b, o_bz_b axes induced by actuator faults, $\bar{T}$, $\bar{L}$, $\bar{M}$, $\bar{N}$ are mean values of the control force and moments. If $\Gamma=[0\ 0\ 0\ 0]$, it corresponds to the situation with no fault in actuators. Then the possible varying range of the components of Γ are given by: $\gamma_T\in[0,\ 0.3]$, $\gamma_L\in[0,\ 0.2]$, $\gamma_M\in[0,\ 0.2]$, $\gamma_N\in[0,\ 0.05]$.

3.2 Nominal Controller Design

In this section the nominal controller will be designed with the structured H_∞ approach. The design is based on the nominal model of the transition flight. That is to say, in the design model $\Gamma=[0\ 0\ 0\ 0]$.

3.2.1 Structured H_∞ Theory

Structured H_∞ is an approach that is able to solve the H_∞ optimization problem with constraints on the structure and the order of the controller. The main idea is to shape the sensitivity functions of the closed-loop system. The transfer functions to be shaped in this paper are the sensitivity function and the control sensitivity function. The sensitivity function is represented as $S(s)=(I+G(s)K(s))^{-1}$ and the control sensitivity function is expressed as $R(s)=K(s)S(s)=K(s)(I+G(s)K(s))^{-1}$. As shown in

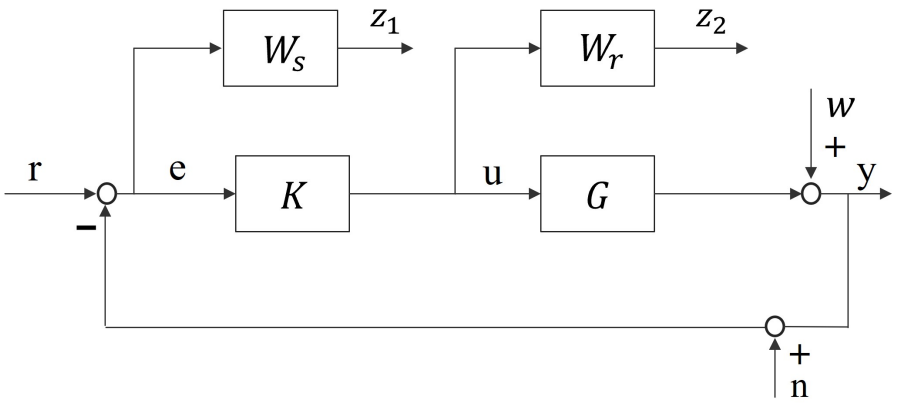

Figure 2 – The general block diagram of a closed-loop system.

Figure 2, the sensitivity function is the transfer function from the disturbance w and reference signal r to the error e. In practice, actuators can provide limited control authority and it is not possible to require a control action that is beyond the actuator capabilities. To the purpose of the design requirements for performance as well as the moderate control actions, weighting functions denoted as $W_s(s)$ and $W_r(s)$ are respectively applied to the sensitivity function and control sensitivity function of the closed-loop system. To this end, the structured H_∞ synthesis problem can be formulated as the following optimization problem for the given control structure:

$$\min_{k\in K} \gamma \tag{10}$$

subject to:

$$\left\| \begin{matrix} W_s(s)S(s) \\ W_r(s)R(s) \end{matrix} \right\|_\infty \leq \gamma \tag{11}$$

where K is the set of considered structured controller.

3.2.2 Control Synthesis

In this section, the attitude and altitude loops control synthesis are detailed. Since the design of attitude control loops including roll channel, pitch channel and yaw channel are pretty similar to each other, only the pitch angle control loop will be further introduced. The altitude control loop that is responsible for holding the altitude of the aircraft constant is designed not only to satisfy the command tracking requirement but also to tolerate the aerodynamic disturbance from the wing. Firstly, the forms of the weighting functions are given. Then the control structures and the weighting functions selection for the pitch angle control loop and altitude hold loop are respectively explained.
The weighting functions $W_s(s)$ and $W_r(s)$ have the following forms:

$$W_s(s) = \frac{s/M + \omega_b}{s + A\omega_b} \tag{12}$$

$$W_r(s) = \frac{r_{max}/u_{max}s + \omega_a 10^{-3}}{s + \omega_a} \tag{13}$$

where M is the peak value of frequency response of the reciprocal of the weighting function that corresponds to the overshoot requirement for time-domain response of the control error, A is the maximum steady-state error requirement, ω_b is the desirable bandwidth of the closed-loop system. r_{max} is the upper limit of the reference signal, u_{max} is the maximum control action within actuators' capabilities, ω_a is the bandwidth of actuators.
Regarding the pitch angle control loop, the control block diagram is shown in Figure 3. The weighting functions are respectively applied to the control error and the pitch control moment. Since the overshoot requirement for time domain response is set to be less than 20%, M is selected as 1.096, the

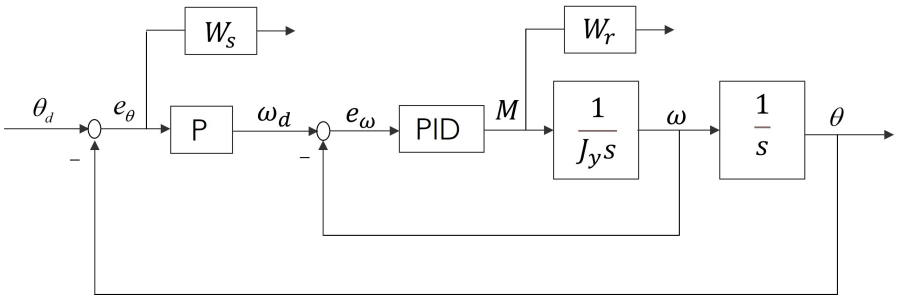

Figure 3 – The control block diagram of the pitch angle control loop.

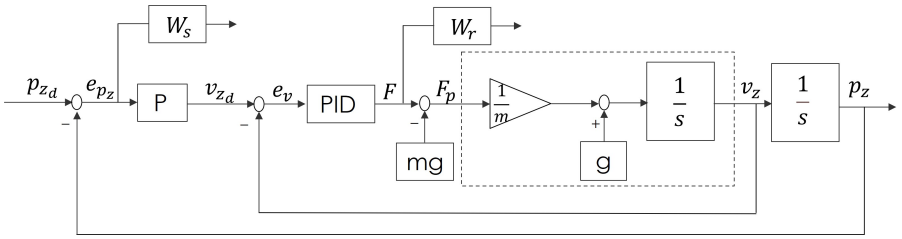

Figure 4 – The control block diagram of the altitude hold loop.

bandwidth ω_b is chosen as 4.3 rad/s according to the settling time requirement 1.2s. A, corresponding to the requirement for the steady state error, is set as 0.001. For the control sensitivity weighting function, ω_a is determined as the bandwidth of actuators that is 5 rad/s.
As for the altitude hold loop, the control structure is almost the same with the pitch angle control loop that is a two layers cascaded PID loop (see Figure 4). The weighting functions are applied to the control error and the thrust force required by the PID controller. Other than the bandwidth frequency of the sensitivity function that is selected as 0.8 rad/s by selecting the settling time as 6s, the other parameters for the weighting functions are given the same values as the pitch angle control loop since the design requirements are the same.

4. Stability and Performance Analysis with Actuator Faults

In the previous section, the control synthesis based on nominal model of the transition flight is conducted. Accordingly, a set of nominal controllers for attitude and altitude control is obtained. However, the preceding control synthesis involves no occurrence of possible actuator faults. Therefore, whether the obtained control system can tolerate a certain degree of actuator faults is not guaranteed. In other words, whether our control system is able to maintain its stability and performance under certain adverse effect from unknown actuator faults or not needs to be checked. In this part, firstly the stability of the developed control system under one propeller partial loss that is equivalent to loss effectiveness of the control force and moments is evaluated. The stability analysis is based on μ-analysis. Subsequently, the performance of the control system is further analyzed. The analysis is carried out exploiting the multi-model approach, where both perturbed sensitivity function and time domain response are analyzed.

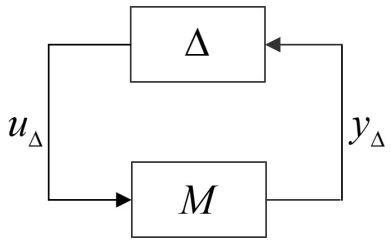

Figure 5 – $M-\Delta$ structure for stability analysis.

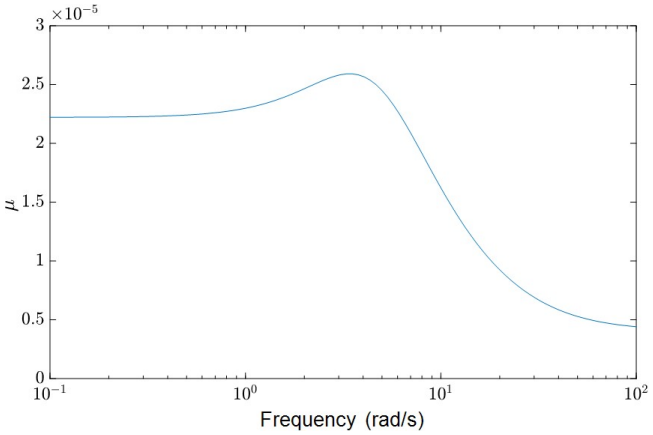

Figure 6 – The μ plot of the pitch angle control loop.

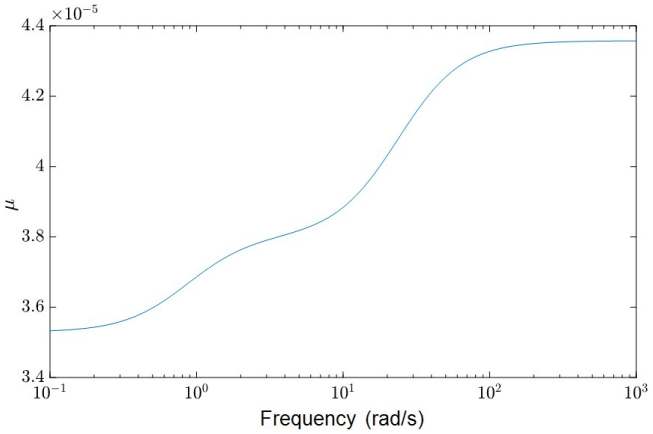

Figure 7 – The μ plot of the altitude control loop.

4.1 Stability Evaluation based on μ-analysis

The structured singular value is an analysis tool that facilitates to help us know the stability of the given control system with a set of perturbed models without need to search through the whole set. With reference to Figure 5 it has the following definition:

$$\mu(M) = \frac{1}{min\{k_m | det(I - k_m M\Delta) = 0\}} \tag{14}$$

where k_m is a scaling factor of uncertainty, $\Delta = diag\{\Delta_i\}$ denote a set of complex matrices with $\bar{\sigma}(\Delta) \leq 1$. Then the sufficient and necessary condition that the $M - \Delta$ system in Figure 5 is stable for all structured perturbations is given by:

$$\mu(M(j\omega)) \ < \ 1, \ \ \forall\omega. \tag{15}$$

Here we consider the stability of the control system with all the possible models in the uncertain model set. This means we talked about the uncertain model given in Section 3.1with the range of Γ: $\gamma_T \in [0,\ 0.3]$, $\gamma_L \in [0,\ 0.2]$, $\gamma_M \in [0,\ 0.2]$, $\gamma_N \in [0,\ 0.05]$. Since the μ plot of attitude loops are pretty similar to each other, so here only the μ plot of the pitch angle control loop and vertical position hold loop are presented (see Figure 6 and Figure 7). It is known from both of the μ plots of the pitch angle and altitude control loops that the μ values are in the level of 10^{-5} respectively in the frequency ranges 0.1-100 rad/s and 0.1-1000 rad/s, which are far less than 1. Thus, according to the preceding robust stability condition, we can know that the control system has good robust stability to the considered actuator faults.

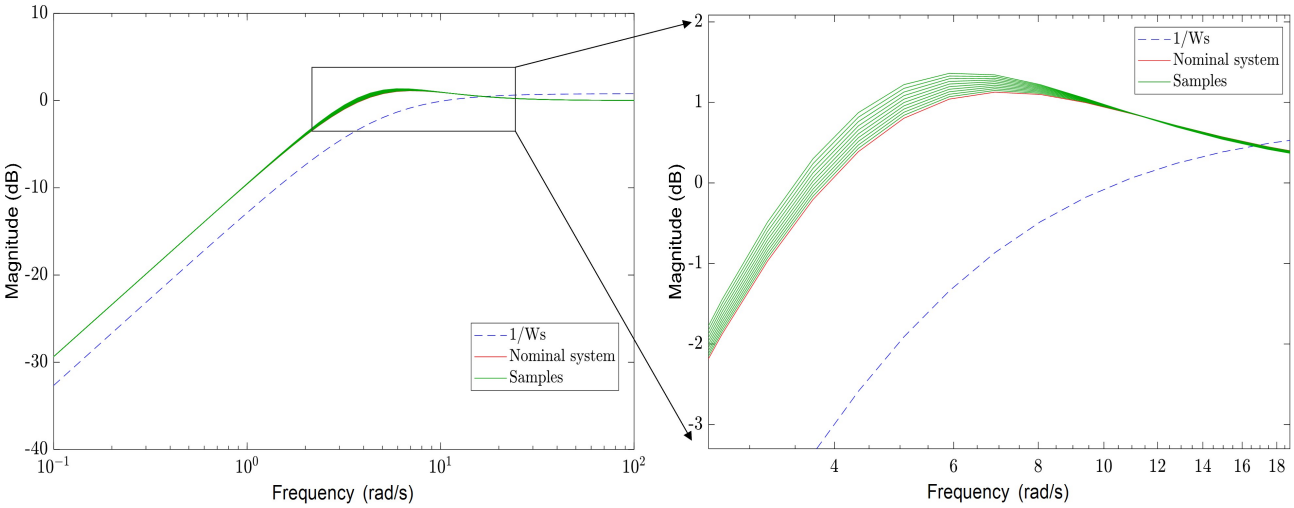

Figure 8 – The frequency response of the perturbed sensitivity functions of the pitch angle control loop.

4.2 Performance Analysis based on Multi-model

In the previous section, the stability of the control system under actuator faults has been analyzed. Accordingly, the performance of the control system with the occurrence of actuator faults will be evaluated in this section. The analysis is based on the discrete multi-model approach from the perturbed sensitivity functions and the time domain response point of view.

Specifically, for the pitch angle control loop the perturbed sensitivity functions are obtained by considering 10 models for different values of γ_M in the interval $[0,\ 0.2]$. As shown in Figure 8, frequency response of the reciprocal of the weighting function and the perturbed sensitivity functions are given. It can be seen that the perturbed sensitivity functions are almost lie below the reciprocal of the weighting function. There is slight violation of the perturbed sensitivity functions against the weighting function. Then we further check the step response of the multi-models obtained by discretizing γ_M with a interval of 0.02. From Figure 9, we can see that maximum overshoot is 1% which is much less than our design requirement 20% for overshoot. The steady state error is 0.001 that satisfies the requirement for steady state error as well. As for the altitude control loop, the frequency response of the perturbed sensitivity functions and the step response are given in Figures 10 and Figure 11. It is noted that the frequency response of the perturbed sensitivity functions lies below the selected weighting function, which illustrates with the obtained control parameters in nominal control design the performance of the perturbed systems still satisfies the design requirement. In the figure of the step response, we can know that there is no overshoot. The steady state error is 0 which is less than 0.001. The settling time is approximately 6s. Generally speaking, even if there is slight violation of the perturbed sensitivity functions against the design weighting function for pitch control loop, the time domain response of both pitch and altitude control loops still satisfies the design requirements.

5. Fault Tolerant Control Simulation

In the previous sections the nominal controller without considering the actuator fault has been developed and its stability and performance under assumed partial loss of a single propeller has been evaluated. The analysis demonstrates the capability of fault tolerance of the developed control system. In this section, the designed control system is further validated on the nonlinear six-degree-of-freedom simulator established in the Matlab-Simulink environment. Two different scenarios of actuator fault are considered: one is the partial loss of propeller 1a, another is the partial loss of propeller 2b (see Figure 1). For both cases, two different levels of loss in effectiveness of propellers are compared to the nominal case. The trajectory in longitudinal plane and time histories of the attitude variation are presented and analyzed, which illustrate the effectiveness of the developed passive fault tolerant control system for the transition flight of the dual-system UAV. On the other hand, since the aerodynamic terms have been negnected in the control-oriented model, the simulation through the nonlinear

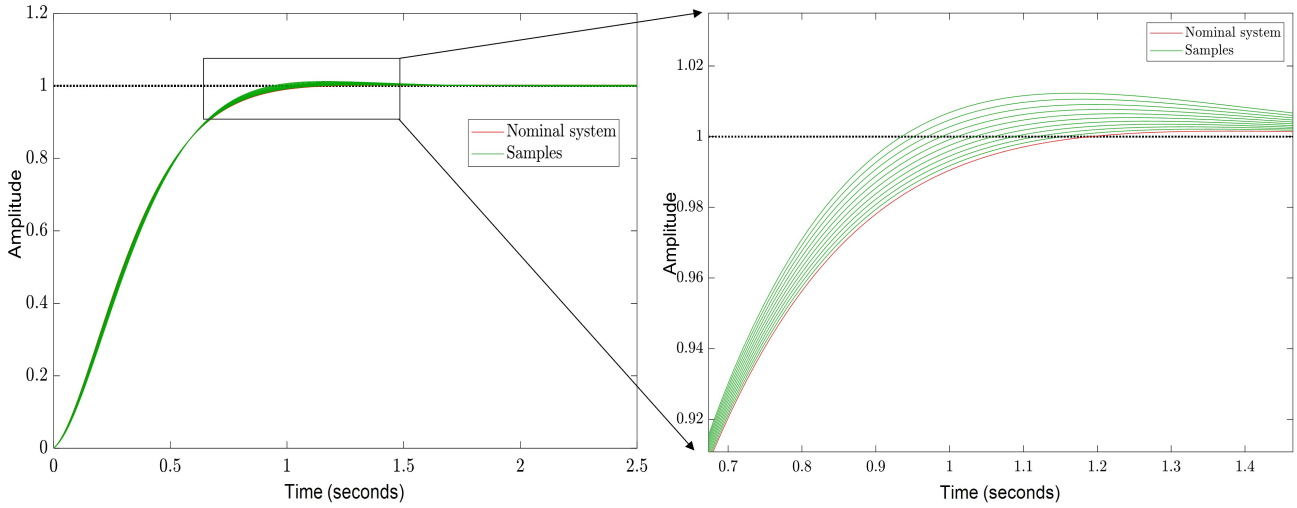

Figure 9 – The step response of the pitch angle control loop based on multi-model.

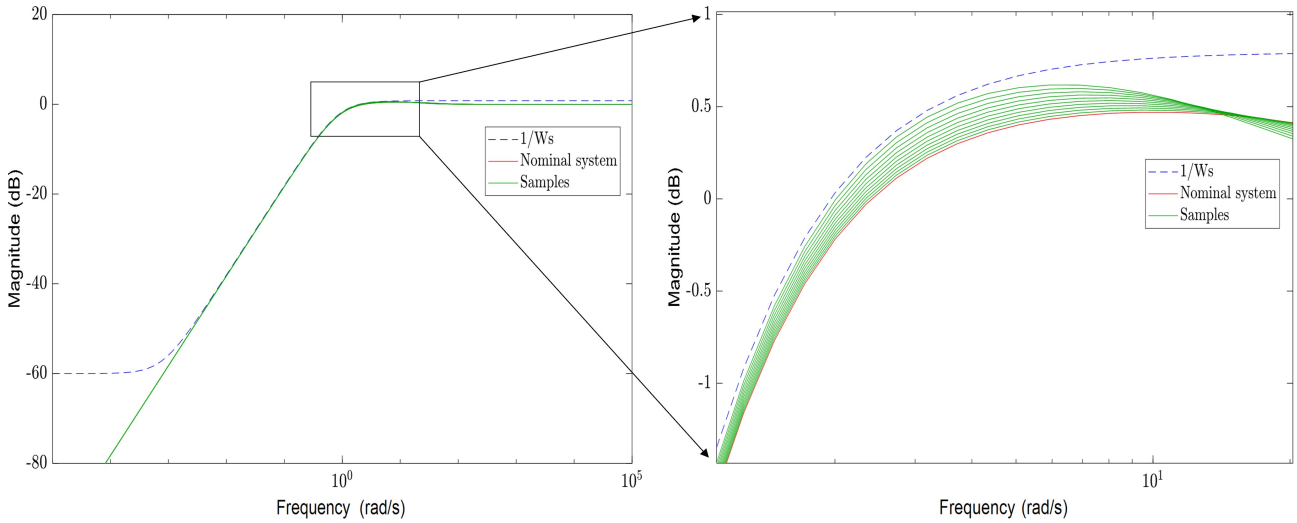

Figure 10 – The frequency response of the perturbed sensitivity functions of the altitude control loop.

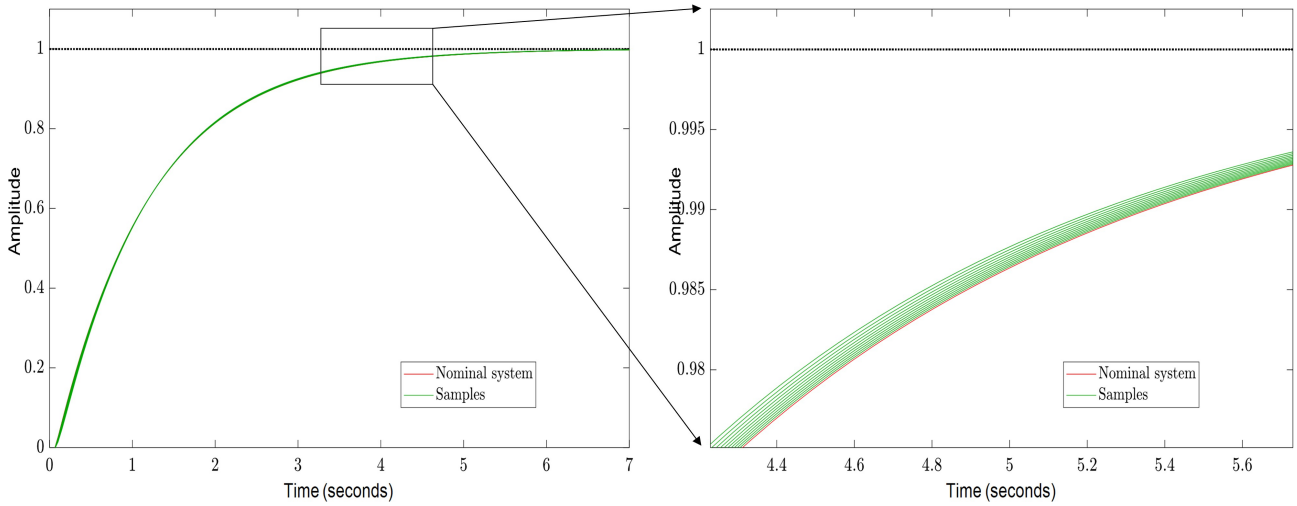

Figure 11 – The step response of the altitude control loop based on multi-model.

simulator also verifies the robustness of the control system to the modeling uncertainties.

5.1 Case 1: partial loss of the propeller 1a

Firstly, we consider the fault scenario of partial loss of the propeller 1a. The dual-system UAV enters transition flight after the hovering in multicopter mode. The simulation scenario is set up by assuming the UAV is in normal flight since 20 seconds in the absence of any fault then a partial loss fault of the propeller is injected at 22 seconds. To be precise, 50% and 30% partial loss of effectiveness of propeller 1a are respectively assumed during the transition flight. The completion time of the transition flight has minor differences depending on the fault scenarios, which are 28.2s, 27.7s and 27.3s respectively corresponding to scenarios of no fault, 30% loss of a propeller and 50% loss of a propeller. Here the time histories of the transition flight as well as the fixed wing flight after transition are presented. The trajectory in longitudinal plane and the time histories of attitude variation are presented in Figure 12. During transition flight, the altitude set point is 30m, as can be seen from the trajectory in longitudinal plane, the altitude variation has minor differences with the loss of effectiveness in propeller increasing. The maximum altitude variation is 0.6m. Finally, the altitude converges to the set point 30m. As for attitude variation the set points are 0. The changes of attitude angles become larger as the percentage of loss increasing. For the roll and yaw angles, the maximum variations are within 2 degrees and that of the pitch angle is less than 4.5 degrees during the transition flight. After that, the attitude variations are further tackled by the fixed wing controller that makes the attitude angles converge respectively to 0, 0.8 degrees, 0. The control system is able to maintain the attitude stable after the adverse effect caused by the actuator fault. Therefore, the simulation results indicate that the developed control system can maintain the transition flight with almost constant altitude and stable attitude even if in the meanwhile there is occurrence of the fault in the propeller 1a.

5.2 Case 2: partial loss of the propeller 2b

Based on the above presented simulation results, we further consider a fault of propeller 2b. The simulation scenario is the same with the previous section. Again, two percentages of loss, namely 30% and 50%, in propeller 2b are assumed. The simulation results under the fault of propeller 2b and no fault are reported and compared in Figure 13. It can be seen from the figures that the variations of the altitude and attitude angles increase as the percentage of loss in the propeller 2b increases. The maximum altitude change is 0.6m and the maximum variation of attitude angles are 5.4 degrees. The simulation results with assumed faults in the propellers 1a and 2b are pretty similar to each other, which once again verifies the passive fault tolerant capability and the robustness to the modeling uncertainties of the designed control system with structured H_∞.

6. Conclusions

This paper is mainly related to the application of structured H_∞ to the transition flight of a dual-system UAV. Based on the control-oriented model the nominal control synthesis including attitude control loops and altitude control loop is carried out with control parameters of the cascaded PID loops obtained from structured H_∞. In the design phase, actuator fault is not considered. Then, the proposed control system is analyzed from the perspective of stability and performance by assuming the occurrence of partial loss of single propeller. The analysis results show that the designed control system is able to maintain stability and performance under the given actuator fault. It is followed by a validation on the nonlinear simulator that demonstrates the passive fault tolerance ability of the control system. The proposed control system for the transition flight of the dual-system UAV is capable to overcome a certain degree of fault in single propeller as well as the modeling uncertainties, which effectively improves the safety and reliability of the transition flight. In view of the essence of passive fault tolerant control, the proposed control system has the advantage of no need for fault information. At the same time, this research is only limited to the discussion of partial loss of single propeller. In future, other fault scenarios like complete loss of a propeller or simultaneous faults of different propellers will be interesting extensions of this research.

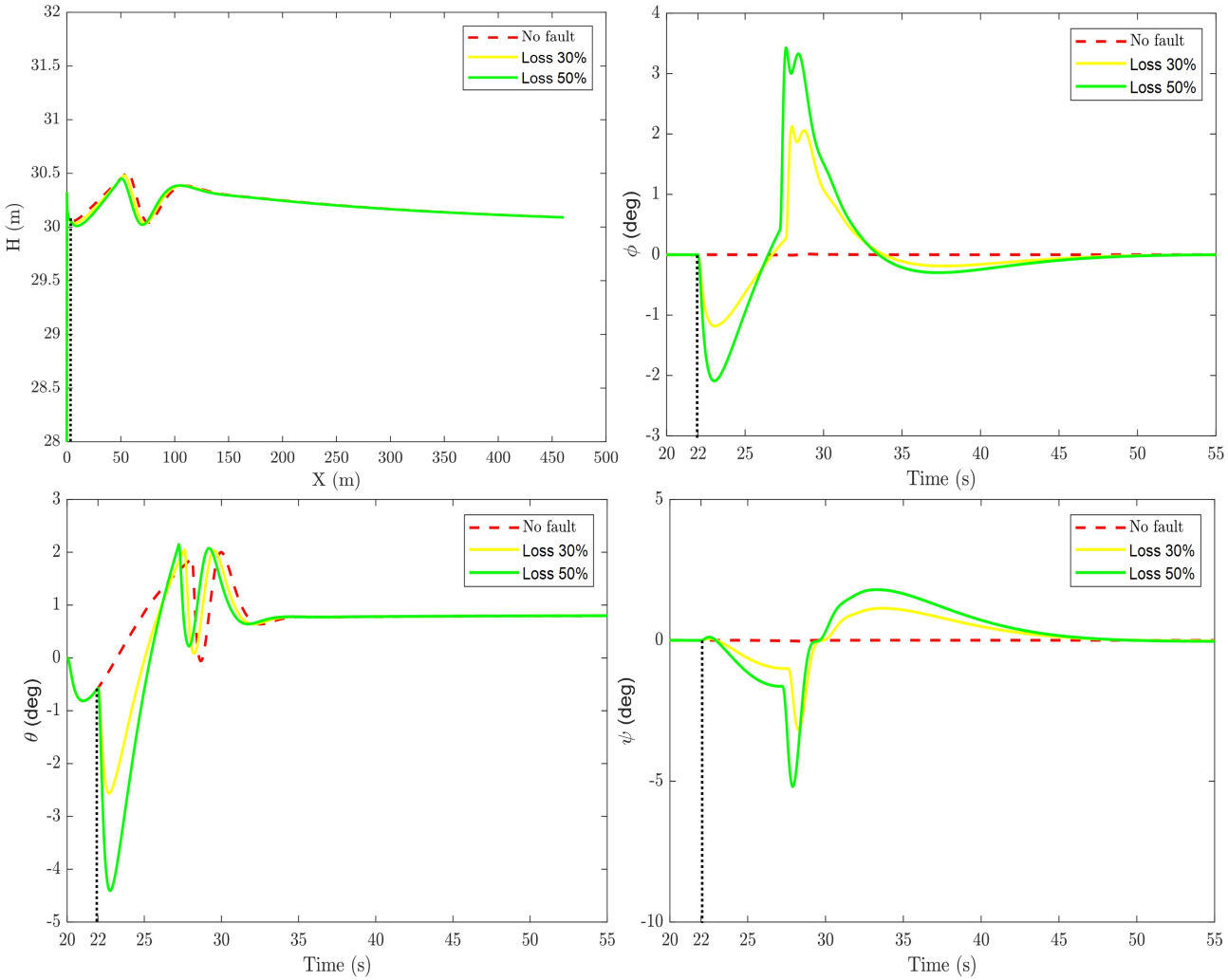

Figure 12 – Trajectory and attitude variations under partial loss of propeller 1a. H, X denote altitude and horizontal position. ϕ, θ, ψ are respectively roll, pitch and yaw angles.

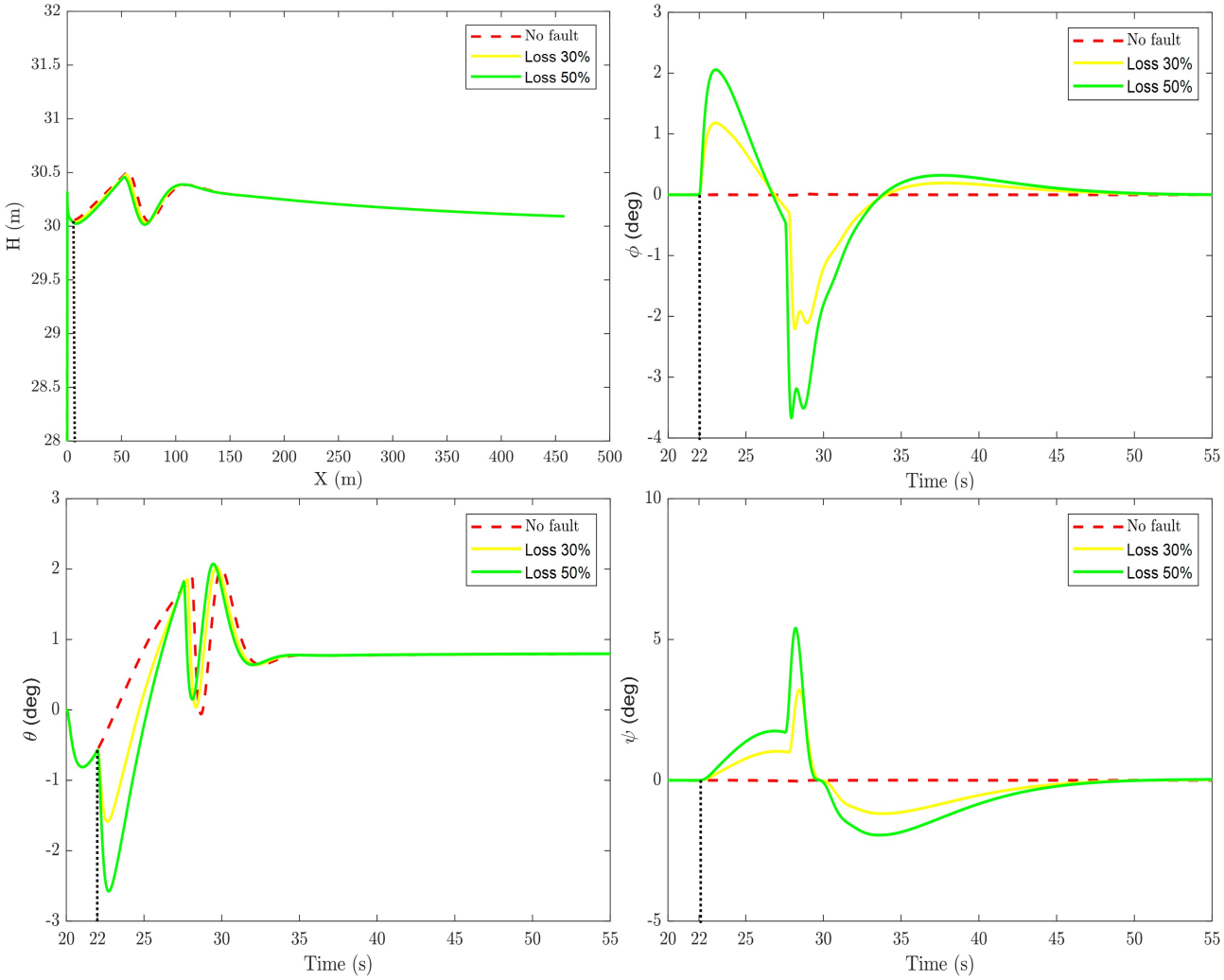

Figure 13 – Trajectory and attitude variation under partial loss of propeller 2b. H, X denote altitude and horizontal position. ϕ, θ, ψ are respectively roll, pitch and yaw angles.

7. Acknowledgment

The first author acknowledges the financial support from China Scholarship Council (No.202006020041).

8. Contact Author Email Address

Mailto: junfeng.cai@polimi.it
Mailto: marco.lovera@polimi.it

9. Copyright Statement

References

[1] Hassanalian M, Abdelkefi A. Classifications, applications, and design challenges of drones: A review. *Progress in Aerospace Sciences*, Vol. 91, pp 99–131, 2017.

[2] Li Z, Zhang L, Liu H, et al. Nonlinear robust control of tail-sitter aircrafts in flight mode transitions. *Aerospace Science and Technology*, Vol. 81, pp 348-361, 2018.

[3] Gai W, Zhang J, Huang L, et al. Transition flight control using adaptive neutral network dynamic inversion for canard rotor/wing UAV. *The 26th Chinese Control and Decision Conference (2014 CCDC)*, China, pp 4210-4214, 2014.

[4] Lu Z, Li H, He R, et al. Energy-Efficient Incremental Control Allocation for Transition Flight via Quadratic Programming. *International Conference on Guidance, Navigation and Control*, Singapore, pp 4940-4951, 2022.

[5] Wang B, Zhu D, Han L, et al. Adaptive fault-tolerant control of a hybrid canard rotor/wing UAV under transition flight subject to actuator faults and model uncertainties. *IEEE Transactions on Aerospace and Electronic Systems*, 2023.

[6] Prochazka K F, Stomberg G. Integral sliding mode based model reference FTC of an over-actuated hybrid UAV using online control allocation. *2020 American Control Conference (ACC)*, USA, pp 3858-3864, 2020.

[7] Wang X, Sun S. Incremental fault-tolerant control for a hybrid quad-plane UAV subjected to a complete rotor loss. *Aerospace Science and Technology*, Vol. 125, pp 107105, 2022.

[8] Nguyen D T, Saussié D, Saydy L. Universal adaptive fault-tolerant control of a multicopter UAV. *IFAC-PapersOnLine*, Vol. 53, No. 2, pp 9340-9347, 2020.

[9] Marcos A. Revisiting the aircraft C* control law: A comparison between classical and structured H-infinity designs. *2017 IEEE Conference on Control Technology and Applications (CCTA)*, USA, pp 2114-2119, 2017.

[10] Weiser C, Ossmann D. Fault-Tolerant Control for a High Altitude Long Endurance Aircraft. *IFAC-PapersOnLine*, Vol. 55(6), pp 724-729, 2022.

[11] Panza S, Lovera M. Rotor state feedback in helicopter flight control: Robustness and fault tolerance. *2014 IEEE Conference on Control Applications (CCA)*, France, pp 451-456, 2014.

[12] Güçlü A. Designing autopilot and guidance algorithms to control translational and rotational dynamics of a fixed wing VTOL UAV. Ph.D. dissertation, Graduate School of Natural and Applied Sciences, Aerospace Engineering, Middle East Technical University, 2020.

[13] Skogestad S, Postlethwaite I. *Multivariable feedback control: analysis and design*. 2nd edition, John Wiley and Sons, 2005.

[14] Härkegård O. Backstepping and Control Allocation with Applications to Flight Control. Ph. D. thesis, Linköping University, Linköping, 2003.